SpaceOps-2023, ID # 93

DESIGN OF REUSABLE ROCKET ENGINE

By Saqer Said Mohammed Al-Rusheidi

Abstract

Since the establishment of MBRSC in 2006, well-heard worldwide breakthroughs have been made in Space field, starting from the manufacture of the first Emirate made satellite to the Mars Hope Probe. These accomplishments are the pride of not just the Emirates, but for the whole region of the Middle East and the Arab world. With such an endless effort of those dedicated workers in MBRSC, it is a guaranteed that we can go even further in achieving the Vision of Sheikh. Mohammed Bin Rashid and his blessed plan to explore the space. With this in mind, this paper is the starting point for a comprehensive study to serve MBRSC's Objectives. The main purpose of this study is to create the first reusable rocket engine capable for landing and take-off on the surface of the red Planet in the Middle East region. In saying that, the author of this paper sets his mind and intention to develop- through continuous study and experiments, a well-established design that encompasses Engine cycle, Retro-Propulsion system and Propulsion feed system.

The design of a reusable rocket engine is a complex and challenging task that requires a thorough understanding of various physical and engineering principles. The engine is the most critical component of a rocket and must meet specific requirements to ensure successful operation. The design process involves the selection of appropriate materials, the determination of geometric parameters such as chamber length, diameter, and nozzle shape, and the analysis of fluid mechanics and heat transfer processes. In this study, the design of a reusable rocket engine that utilizes liquid oxygen and Methane as propellants was investigated. The objective was to meet the technical specifications while also considering factors such as cost, reliability, and ease of maintenance. The results of the design analysis were evaluated and compared to existing reusable rocket engine designs. The study provides a comprehensive overview of the design process and includes recommendations for future work to further improve the design and performance of reusable rocket engines.

Keywords: LOX/Liquid-Methane Rocket Engine, pintle injector, planetary landing, Retro-Propulsion, Regenerative Cooling,

Nomenclature

NO	symbol	Description	unit
1	μ	Dynamic viscosity	$Kg/m.s$
2	M	Molecular	$1/n$
3	C_p	Specific heat	$KJ/Kg.K$
4	γ	Gammas	-
5	k	Thermal conductivity	$W/m.K$
6	μ_ω	Kinematic viscosity	m/s^2
7	T_{aw}	Adiabatic flame Temperature	K
8	T_{wc}	Chamber inner wall Temperature	K
9	T_{co}	Coolant Temperature	K
10	T_{gw}	Gas-wall Temperature	K
11	h_g	Coefficient of Heat Transfer gas said	$W/m^2.K$
12	h_c	Coefficient of Heat Transfer fluid said	$W/m^2.K$

13	h_w	Coefficient of Heat Transfer wall said	$W/m^2.K$
14	q	Conductive heat transfer	$W/m^2.K$
15	P_C	Chamber pressure	bar
16	T_C	Chamber temperature	K
17	A_e/A_t	Exit to throat area ratio	-
18	C*	C star	m/s
19	C_f	thrust coefficient	-
20	I_{vac}	Vacuum specific impulse	s
21	I_{sp}	Sea level Specific Impulse	s
22	R_t	throat radius	m
23	A_t	throat area	m^2
24	F	Thrust	KN
25	$\cup_c$	Chamber specific volume	m^3/Kg
26	$\cup_t$	Nozzle throat volume	m^3/Kg
27	$\cup_e$	Nozzle exit volume	m^3/Kg
28	v_e	Exit gas speed	m/s
29	$\dot{m}$	Mass flow rate	Kg/s
30	$\dot{m}_o$	Oxidizer mass flow rate	Kg/s
31	$\dot{m}_f$	Fuel mass flow rate	Kg/s
32	A_c/A_t	Chamber to throat area ratio	-
33	A_c	Chamber area	m^2
34	R_c	Chamber radius	m
35	D_c	Chamber dimeter	m
36	V_c	Chamber volume	m^3
37	L_c	Chamber length	m
38	L_1	Length from chamber to throat	m
39	R	universal gas constant unit	$m^3 \cdot Pa \cdot K^{-1} \cdot mol^{-1}$
40	C	specific speed	m/s
41	ϵ_c	chamber to throat area ratio	-
42	t_s	resident time	s
43	Cd	discharge coefficient	-
44	Loben		m
45	d_o	oxidizer inject dimeter	m
46	d_f	fuel inject dimeter	m

47	α	spray angel	deg
48	P_r	turbulent flow	-
49	ρ	density	Kg/m^3

.

1. Introduction

Designing a reusable rocket engine for long-duration missions, such as a landing on Mars, requires a detailed understanding of the various components of the engine and how they interact with one another. The design must also take into account the harsh conditions of space travel, including high temperatures, extreme pressure, and vibration. One of the most important considerations in the design of a reusable rocket engine is the use of regenerative cooling. This involves circulating a coolant, such as liquid hydrogen, through the engine's walls to absorb heat and prevent overheating. Another important consideration is the design of the injector, which is responsible for introducing fuel and oxidizer into the engine's combustion chamber. The injector must be able to withstand high temperatures and pressures, and be able to provide a precise and stable mixture of fuel and oxidizer. The engine's nozzle also plays a critical role in the overall performance of the engine. The nozzle's shape, known as its contour, must be designed to optimize the expansion of exhaust gases and generate the maximum thrust possible. Other key factors that must be taken into account in the design of a reusable rocket engine include the thrust chamber's size and shape, the mass flow rate of the fuel and oxidizer, and the specific volume of the engine's combustion chamber. In order to ensure the success of a long-duration mission, it is important that the engine's design is thoroughly tested and validated through a series of ground and flight tests. Only then can the engine be considered reliable and ready for use in a real-world mission.

I. Problem Statement

Historically, cryogenic rocket engines have not been used for long term in-space applications due to their complexity, the mission requirement for high reliability and the challenges associated with propellant boil-off and ignition. On the other hand, cryogenic rocket engines offer the potential for higher performance and greater mission flexibility.

II. Why LO2/LCH4?

Liquid oxygen and liquid methane are leading options for space propulsion systems requiring high propellant bulk density, low-toxicity and similar thermal management characteristics. For the majority of applications, the benefit resulting from smaller, lighter tanks and low boil-off losses counterweight the disadvantage in terms of theoretical specific impulse, for instance, if compared to the liquid oxygen/liquid hydrogen propellant combination. Compared to highly toxic space storable propellants, such as N2O4 and UDMH, oxygen and methane can be more easily handled, leading to a substantial reduction in the operational costs. Besides, due to the presence of methane in the Martian atmosphere, the possibility of in-situ production through, e.g., the Sabatier process, for long duration missions is envisioned the possibility of in-situ production places methane as the preferred fuel on Mars. Other hydrocarbon fuels such as methanol, ethanol and aromatic hydrocarbon blends can also possibly be produced on Mars, but most studies and technology development activities have focused on methane. Despite the aforementioned advantages, cryogenic storage in space still poses some problems. These issues might be partly remedied by, for example, passive techniques, such as shielding and spacecraft orientation, or active means, such as refrigeration to keep propellants within the liquid range. Additionally, among all hydrocarbon fuels, methane possesses the lowest heat capacity as a liquid. As a result, regenerative cooling can only be affected at supercritical pressures (above ca. 45.8 [MPa] for methane) where problems of boiling heat transfer can be avoided. (1)

III. Additive manufacturing

Additive manufacturing is a fast-growing technology that is now being explored for use in space flight applications. Rocket engine components are usually complex in design, take long fabrication times, and are costly to manufacture using conventional manufacturing techniques. Additive manufacturing has the potential to overcome those disadvantages by offering reduced cost, faster fabrication times, and design flexibility not limited by conventional manufacturing. Certainly, the additive process still faces challenges that inhibit extended use for component fabrication (e.g., rough surface finish, porosity, etc.). Nevertheless, as the technology improves, additive

manufacturing could provide a significant advantage for rocket engine design. Consequently, future versions of the engine will explore how to successfully incorporate components that are created using additive manufacturing. (2)

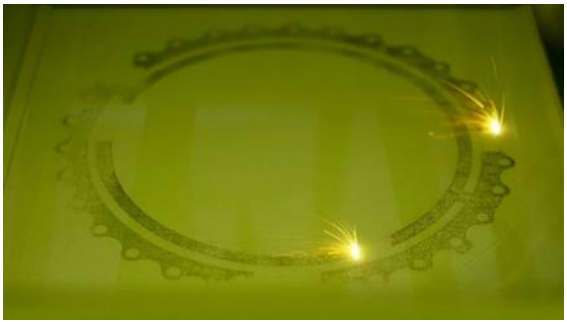

Picture 1.1: Laser sintering a component with internal design features

IV. What is Retro-Propulsion?

Advanced robotic and human missions to Mars require landed masses well in excess of current capabilities. One approach to safely land these large payloads on the Martian surface is to extend the propulsive capability currently required during subsonic descent to supersonic initiation velocities. However, until recently, no rocket engine had ever been fired into an opposing supersonic freestream. Retro-propulsion decelerates a vehicle by providing thrust opposing the vehicle's direction of motion. So far, it has been mostly used on spacecrafts for de-orbit maneuvers, to slow the final landing approach and to cushion the landing impact. A very recent application of retro-propulsion is to decelerate the hyper- and supersonic re-entry phase of a space vehicle, known as supersonic retro propulsion (SRP). Up to date only the privately owned space company SpaceX uses supersonic retro-propulsion to slow down the hypersonic re-entry phase (re-entry burn as they name it) of the returning first stage of their carrier system Falcon 9. (3)

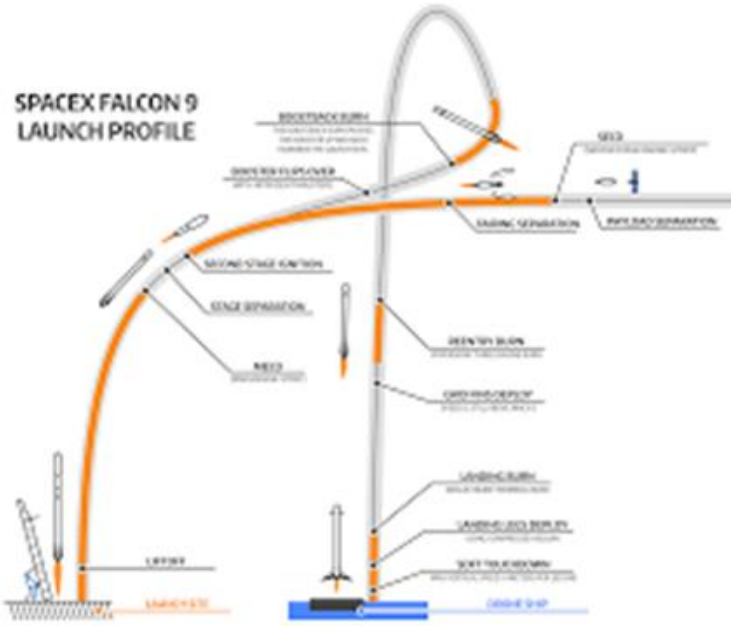

Fig 1.2: SpaceX Falcon 9 Launch Profile (3)

V. Variable-Area Injectors

Of particular interest are those missions involving planetary landing and orbit maneuvers, which usually impose a degree of thrust modulation capability over the propulsion system. Strictly from the standpoint of the thrust chamber injection system, the pintle injector is an attractive choice in this case, due to its inherent combustion stability

characteristics, proven design and simple manufacture. Having being qualified for use with storable, hypergolic propellants, very little design criteria is available for design of pintle type injectors for rocket engines running on LO2/LCH4 propellants.

VI. Scope and Research Goals

This research devotes attention to the design characteristics of a thrust and geometry of engine, also development of Regenerative Cooling and injection systems based on the LO2/LCH4 propellant combination and that additionally offer the potential throttling capability required by planetary landing missions. The primary goal of this research is to broaden the reusable rocket engine technology and to establish engineering database for developing a variable thrust oxygen/methane propulsion system that will deliver:

1. Stable operation;
2. Wide thrust range;
3. High combustion performance.
4. thrust control during throttling for landing impact

VII. Theoretical Performance

The research focused on the theoretical side of design and for that, we must be taken in account The following discussion presents the technique used to estimate propellant performance in terms of attainable specific impulse

1. Recombination (Kinetic) Losses

Because of the high theoretical combustion temperatures (well above 2000 [K]) and the resultant dissociated gas species, it is anticipated that the LO2/LCH4 may have relatively large recombination (kinetic) losses. For the present analysis, the effect of non-equilibrium chemistry was assumed to produce a loss of 1% compared to shifting equilibrium chemistry. (4)

2. Divergence Losses

Divergence loss is essentially a loss due to nozzle geometry in that the gases leave the nozzle exit at some angle with respect to the nozzle axis. The divergence loss coefficient was used as a constant throughout the analysis and set equal to 0.98. (4)

3. Viscous Losses

The combined friction and heat transfer losses which are defined as the viscous losses can be computed using the technique of reference (4). This reference considered the simultaneous solution of the integral momentum and integral energy equations for the turbulent boundary layer in a rocket engine. (4)

4. Zonal Losses

Performance levels are sensitive to variations in mass and mixture ratio distributions across the chamber. This parameter is highly dependent on the cooling approach and injector type used. For this analysis, it was assumed that a maximum of 3% performance losses are present, as long as the central core can be maintained at the global equilibrium mixture ratio. (4)

VIII. Reference Engine

The reference engine was designed to obtain the engine system performance in the sub-scale engine test. The specifications of reference engine are shown in the Table 1. The thrust of 30kN is selected to the reference engine for sub-scale firing test to expect to be applied to any small precursor missions such as reusable vehicle, planet lander, and orbital transfer vehicle.

	HD	MIRA	ACE-42R	BE-4	Raptor	LE-8 engine	30kN-class engine	100kN-class engine
								
Country	USA	Italy	France	USA	USA	Japan	Japan	Japan
Company	NASA	Avio	AIRBUS	Blue Origin	SpaceX	IA/JAXA	IA/JAXA	IHI
Vehicle	Morpheus lunar lander	VEGA Upper stage	Space Plane	Vulcan 1st stage	Interplanetary transport system	-	-	-
Thrust [kN]	24	98	420	2400	3500	107	30	98
Isp vac.[sec]	215	364	340	330	382	315	335	356
Engine Cycle	Pressure Feed	Full Expander	Gas Generator	Staged Combustion	Staged Combustion	Gas Generator	Pressure Feed	Gas Generator
Propellant Feeding	Pressure Feed	Turbo Pump	Turbo Pump	Turbo Pump	Turbo Pump	Turbo Pump	Pressure Feed	Turbo Pump
Chamber Cooling	Film Cooling	Regenerative	Regenerative	Regenerative	Regenerative	Ablative	Ablative	Regenerative

Table 1. LOX/Methane Engine Development (5)

\

2. Material and methods

I. Design Characteristics of a Thrust Chamber:

The thrust chamber assembly consists of combustion chamber, nozzle and igniter. In the thrust chamber, the propellants that come from the feed system are injected, atomized, mixed and burned to turn into hot gases that are ejected at high speeds. By the principle of conservation of energy, it can be understood that in the thrust chamber occurs a conversion of random motion of the molecules at high speeds (heat) into an ordered stream of gas at high speed (kinetic energy). (6). CEA (Chemical Equilibrium and Application) code, developed by NASA, is used to obtain the mixture ratio of the propellants, the temperature and the pressure at the combustion chamber. Equilibrium chemistry in the combustor and full shifting is assumed.

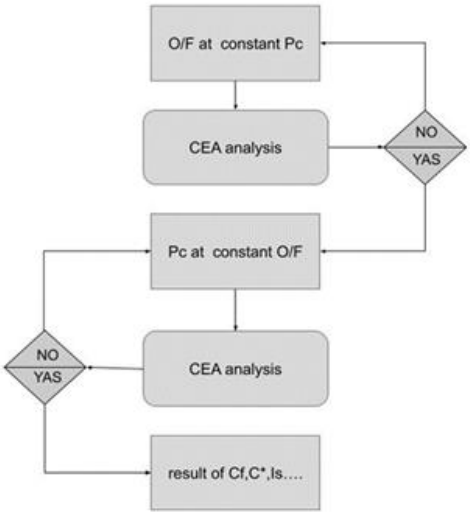

workflow 1.1:data analyse for to obtain MR

Mixture Ratio at 2.8:

The mixer ratio, also known as the fuel-to-oxidizer ratio, is the proportion of fuel and oxidizer that is mixed and burned in a rocket engine. The mixer ratio can affect the performance of a rocket engine in several ways.

When the mixer ratio is increased, more fuel is added to the mixture. This can lead to a higher thrust, as more fuel means more energy is released during combustion. However, increasing the mixer ratio also increases the fuel flow rate, which can lead to an increase in the weight of the engine. Additionally, a higher mixer ratio can also lead to a higher combustion temperature, which can cause thermal stress on the engine's components. On the other hand, when the mixer ratio is decreased, less fuel is added to the mixture. This can lead to a lower thrust, as less fuel means less energy is released during combustion. However, decreasing the mixer ratio also decreases the fuel flow rate, which can lead to a decrease in the weight of the engine. Additionally, a lower mixer ratio can also lead to a lower combustion temperature, which can reduce thermal stress on the engine's components.

This chart 1.1 was generated using CEA. The curve in the chart is not smooth due to rounding errors of decimal places in the results; the results are deemed acceptable for comparison nonetheless. From the chart it can be seen that the optimal MR range varies somewhere around 2.8 to 3.1 (up to pressures of 400 psia). After assessing the data, an MR of 2.8 was selected.

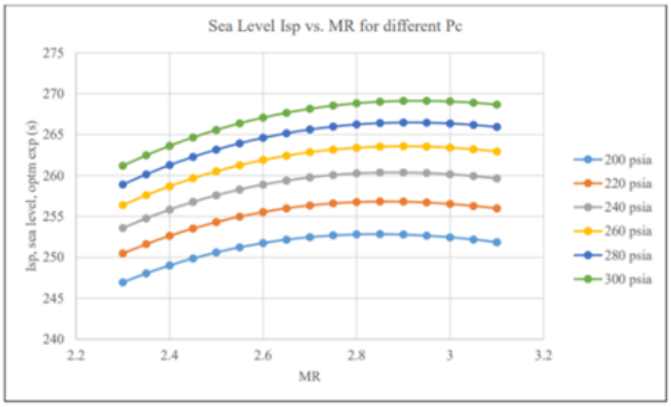

Chart 1.1: Sea Level Isp vs. MR for different Pc

Although a higher MR would theoretically provide higher performance, there are several reasons why an MR of 2.8 would prove beneficial. First, at mentioned pressures and saturation temperature of LOX & LCH4, a ratio of 2.8 leads to equal tank size. This occurs because at those conditions the density of liquid oxygen is approximately 2.8 times greater than the density of liquid methane, leading to equal propellant volume. Equal tank size reduces vehicle complexity because tank design can be similar for both propellants. Second, a higher MR leads to higher combustion temperatures, requiring more cooling. Chart 1.2 demonstrates Tc for different MRs at different combustion pressures.

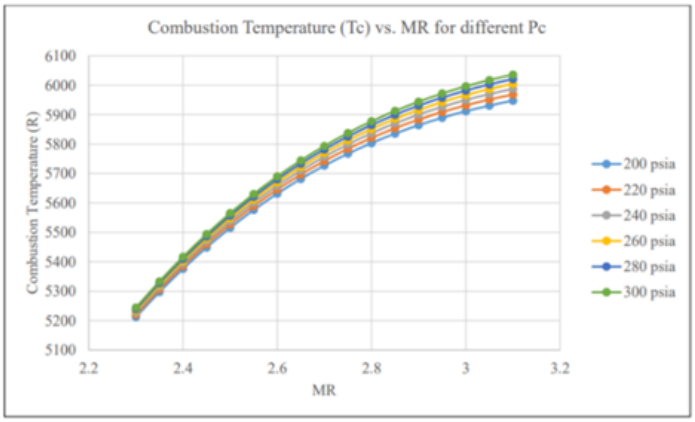

Chart 1.2: Tc vs. MR for different Pc

Chamber pressure is very important in the designing of rocket engine. The thrust chamber performance increases with increase in chamber pressure and also higher chamber pressure reduces the performance losses due to kinetics. Thrust chamber size and weight decreases as the chamber pressure increases. Higher chamber pressure provides higher nozzle expansion ratio, which in turn reduces the chamber and nozzle envelope for a fixed thrust. (7). When the pressure in the chamber is increased, the temperature of the combustion gases also increases. This is because the increased pressure causes the gases to compress, which leads to an increase in the temperature of the gases. As the temperature of the combustion gases increases, the thermal stress on the engine's components also increases. This is because the high temperatures can cause the materials used in the engine's components to expand and contract more, which can lead to cracking and other forms of damage over time.

Additionally, higher combustion temperatures can also lead to a decrease in the performance of the engine. This is because the high temperatures can cause the combustion gases to expand more quickly, which can lead to a decrease in the thrust produced by the engine. Furthermore, high temperatures can cause the nozzle to erode which can decrease the thrust. the pressure of the chamber is a trade-off between thermal stresses on the engine's components and the performance of the engine. Engineers will need to optimize the pressure of the chamber to balance these factors and achieve the best performance for the specific mission.

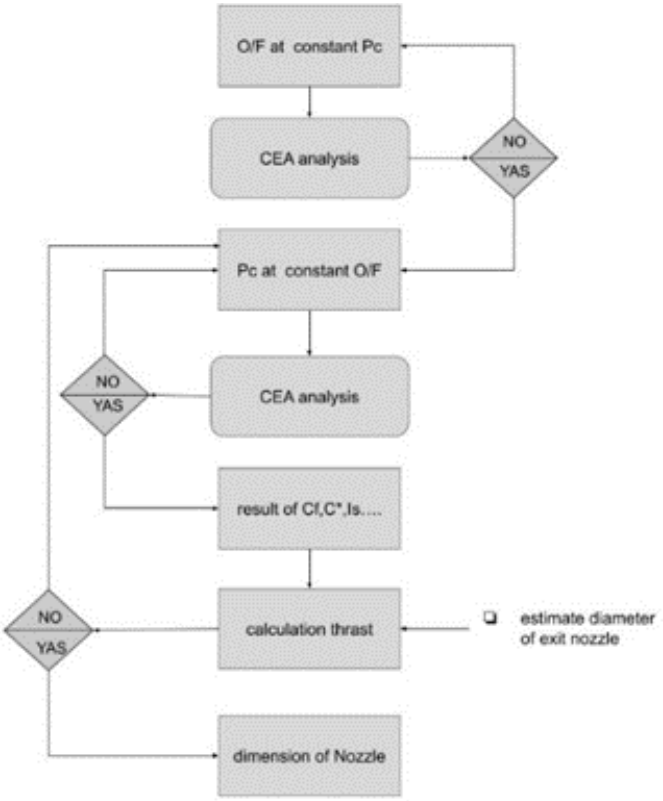

workflow 1.2: data analyses to obtain Pc.

After several data analyses as the workflow diagram shows, the performance parameters are obtained through NASA-CEA code for the given final input condition of the m/r at 2.8 with pressure of 40 bar, temp fuel 110k and oxy at 90k to be applied to any small precursor missions such as reusable vehicle, planet lander, and orbital transfer vehicle. Those values are listed in the following table. Based on the final output value from CEA-Code table 1.2, The thrust of 31kN is obtained by systematic calculation and are summarize specifications thrust throttling in the Tab. 1.3 to meet the engine thrust throttling requirement with dependence on Diameter of exit nozzle as a key factor that controls size and weight and affects propulsion engine.

CEA (Chemical Equilibrium and Application)				
FUEL CH4 162.000 K / OXIDANT O2(L) 90.000 K				
	UNIT	CHAMBER	THROAT	EXIT
Pressure	bar	40	23.002	1.0256
Temp	K	3359.1	3164.83	2058.62
M	1/n	19.562	19.768	20.307
Cp	KJ/KG. K	5.5768	4.9643	2.4478
GAMMAs	-	1.1441	1.1463	1.2050
MACH	-	0	1	2.85
PERFORMANCE PARAMETERS				
Ae/At	-	-	1	6.1
CSTAR	M/SEC	-	1873.9	1873.9
CF	-	-	0.6592	1.533
Ivac	M/SEC	-	2312.9	3166.1
Isp	M/SEC	-	1235.3	2872.7

Table 1.2: CEA Performance Parameters

Parameter	unit	value
F	KN	31.56
Tc	K	3359.1
v_e	m/s	2872.6887
$\dot{m}$	Kg/s	10.98
$\dot{m}_o$	Kg/s	8.09
$\dot{m}_f$	Kg/s	2.89
$\cup_t$	m^3/Kg	0.57
$\cup_e$	m^3/Kg	7.38
D_t	m	0.08
A_t	m^2	0.00514

Table 1.3: Specifications Thrust Throttling

II. The Geometry of Combustion Chamber and Nozzle:

The design of the geometry of a combustion chamber and nozzle plays a crucial role in the performance of a rocket engine. A well-designed combustion chamber and nozzle ensures that the combustion process is efficient, which in turn generates maximum thrust and specific impulse. The design of the combustion chamber and nozzle is based on several factors, such as pressure and temperature, mass flow rate, and geometry. The shape and size of the combustion chamber and nozzle are optimized to ensure that the pressure and temperature of the gases inside the chamber are maintained at levels suitable for combustion. Additionally, the design of the combustion chamber and nozzle should also ensure that the mass flow rate of the gases is maximized, which increases the thrust generated by the engine. In summary, the design of the geometry of a combustion chamber and nozzle is a complex task that requires an in-depth understanding of thermodynamics, fluid mechanics, and heat transfer.

Nozzle design:

The design of a contour type in a rocket engine nozzle can be accomplished using the characteristic method, which uses the properties of the exhaust gases to determine the optimal shape of the nozzle. This method is based on the concept of free expansion of the exhaust gases, which means that the gases are allowed to expand without any additional energy input. The characteristic method involves first determining the thermodynamic properties of the exhaust gases, such as the pressure, temperature, and velocity at the nozzle exit. These properties are used to calculate the ratio of specific heats (gamma) and the specific heat at constant pressure (Cp) of the gases. Next, the

design of the nozzle contour is divided into two parts: the converging section and the diverging section. The converging section is designed to increase the velocity of the exhaust gases, while the diverging section is designed to decrease the pressure of the gases and increase their velocity further. The design of the converging section is based on the concept of isentropic flow, which means that the flow is reversible and adiabatic. The angle of the converging section is determined by the ratio of specific heats and the specific heat at constant pressure of the gases. The design of the diverging section is based on the concept of Fanno flow, which means that the flow is irreversible and adiabatic. The angle of the diverging section is determined by the ratio of specific heats, the specific heat at constant pressure of the gases, and the area ratio of the nozzle.

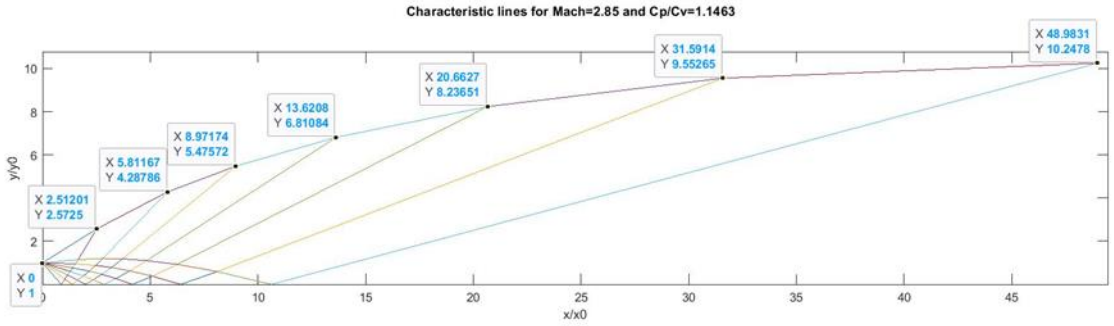

Fig 1.3: Characteristic line for Mach 2.85, Cp/Cv 1.14

The nozzle in Fig. 1.3 is contour type, which was profiled with help of the characteristic method with free expansion of exhaust gases. This shape has better performance and is shorter than conical one, were performed for a number of cases using a computer program developed in MATLAB. This computer program solves the characteristic method equations.

Shock Structures from the Exhaust:
Once the nozzle contour is designed using the characteristic method, it is then tested using computational fluid dynamics (CFD) simulations and wind tunnel testing to ensure that it will perform as expected in flight.
.

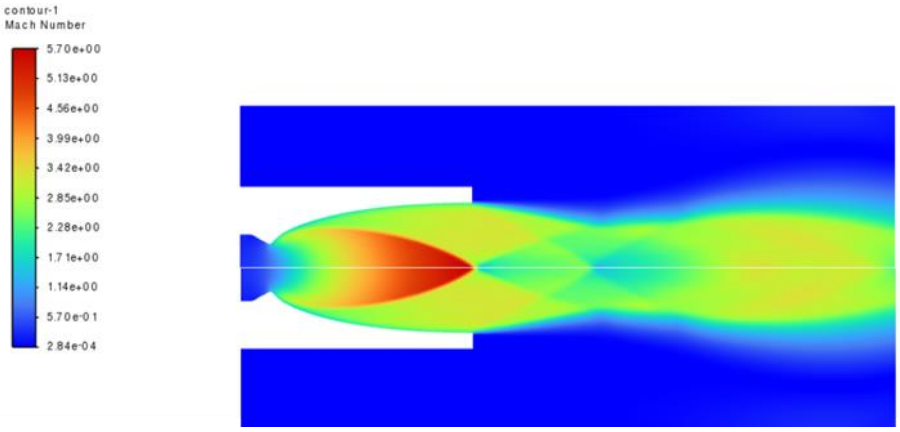

Fig 1.4: Shock structure at nozzle exit

Analysis methodology of CFD with commercial ANSYS fluent used to determining the shock structures from the exit of the rocket nozzle. The figure 1.4 shows the development of the shock near nozzle exit. From the velocity contours obtained, under expanded jet from the nozzle along with the intercepting shock and the reflected shocks are visualized. The above picture dictates the result obtained during the fully developed flow out of the nozzle and gives a clear understanding of how the exhaust jet will behave when the flow expelled out from the nozzle. Here the shock structures are properly formed indicating proper intercepting shock and the reflected shock. The shape of exhaust jet and the shocks in it are studied and further considered for the study of jet and launch pad interactions.

It's important to note that the characteristic method is one of the several design methodologies that can be used for the nozzle contour design, and each method has its own advantages and disadvantages depending on the specific application and the requirements of the rocket engine.

Combustion chamber design

Optimum characteristic length of the combustion chamber of liquid rocket engine is very important to get higher energy from the liquid propellants. Characteristic length is defined by the time required for complete burning of fuel. Combustion reactions are very fast and combustion is evaporation dependent. Characteristic length has normally value between 0.8 and 3 meters. It can be higher in some conditions. Normally characteristic length for a new combustion chamber is selected on the basis of experiments or data available in literature of successful combustion chambers. (8) The design and performance parameters of the thrust chamber are obtained by systematic calculation and are summarized in the Tab. 1.4 The geometry associated with combustion chamber are calculated assume in Characteristic length of 1.1, with future Hot fire test will be revaluated.

Parameter	unit	value
$\cup_c$	m^3/Kg	0.35
$\boldsymbol{A_c/A_t}$	-	3.53
$\boldsymbol{A_c}$	m^2	0.018
$\boldsymbol{D_c}$	m	0.16
$\boldsymbol{V_c}$	m^3	0.0056
$\boldsymbol{L_c}$	m	0.3
$\boldsymbol{L_1}$	m	0.053

Tab. 1.4 The Geometry of Combustion Chamber

III. Heat Exchanger:

The heat exchanger (or cooling system) is responsible to absorb heat from the walls of the thrust chamber in order to prevent the wall material from change phase, i.e., the material can be melted or even evaporated. The most used and efficient for a LRE is the regenerative cooling system where the working fluid (usually the fuel) exchanges heat from the thrust chamber and then the fluid is burned in the combustion chamber. With this cooling system all heat absorbed can be used for purposes of propulsion, hence the name regenerative. (9). Today, the needs for longer and faster space travel require rockets with more powerful thrust and also bring challenging requirements to the cooling system. Much higher heat transfer rate is needed for next generation rockets. Even with new advances in high-temperature and high conductivity materials, thrust increases for large liquid propellant rocket engines are limited by the cooling capacity of the cooling jacket. Cooling limits have been extended with the use of film cooling, injector biasing, and transpiration cooling. However, these methods are costly to engine performance since they require that some of the fuel pass through the thrust chamber throat without contributing to thrust. (10)

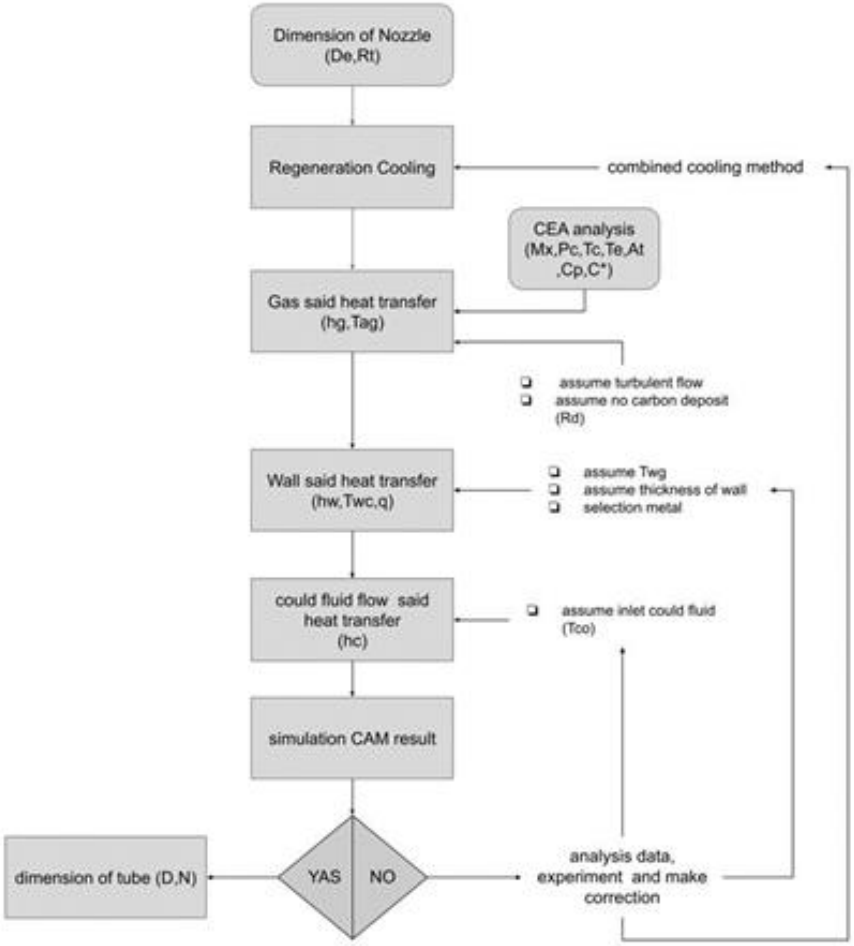

Flowchart 1.2:

Coolant Limitations

Methane requires a limit to the allowable coolant-side wall temperature. Methane can thermally decompose and form the so-called" coke "between a range of temperatures from 1030 to 1370 [K], but since these temperatures are well above the wall temperature limited by structural reasons, no consideration was given in this respect. In this analysis, therefore, a maximum temperature of 590 [K] was taken as the maximum allowable temperature for Stainless-steel materials in contact with methane. The lack of appreciable sub-cooling also limits the channel design. However, the pressure effect is rather strong; for this reason, cooling with methane at high pressures was made without regard to a

bulk temperature limit. For supercritical methane, maximum acceptable fluid velocity was not allowed to exceed a Mach number of 0.3 locally

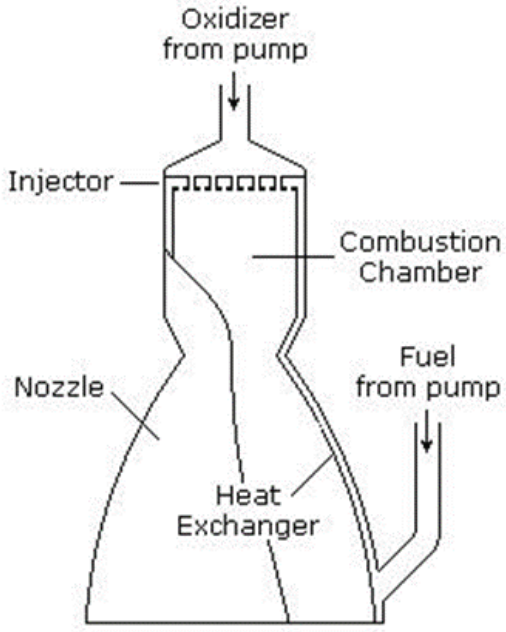

Fig 1.5: regenerative cooling flow diagram

Regenerative Cooling Analysis

Combining the thrust chamber contour, the gas-side heat transfer distribution, thrust chamber material properties (thermal conductivity, yield strength) and the thrust chamber design conditions (propellant properties, thrust, chamber pressure, mixture ratio, coolant flowrate), regenerative cooling analyses were performed for a number of cases using a computer program developed in MATLAB. This computer program solves the steady-state one-dimensional heat transfer equations. and is capable of either designing or evaluating channel wall coolant passages in different configurations

At throat section			
Gas (3164.83 K)	Parameter	unit	value
	μ	Kg/m.s	2.59599E-06
	M	1/n	19.562
	γ	-	1.1463
	C_p	KJ/Kg.K	4.9643
wall	k	w/m.k	13.3
Could fluid (CH4 at 111 K)	μ	Kg/m.s	0.0001213
	μ_w	m^2/s	2.86E-07
	K	w/m.k	0.1841
	C_p	KJ/Kg.K	2.232

Table 1.5:

Program output includes coolant heat input, coolant pressure and bulk temperature distribution and chamber wall temperature profiles. The design of the Stainless-steel chamber liner was based upon the gas- and liquid-side heat transfer correlations. These analyses were used to more accurately determine the regenerative cooling limits and can provide more realistic reference data in the generation of parametric coolant heat input and coolant pressure drop required to perform the engine cycle balances.

At throat section			
Gas (3164.83 K)	Parameter	unit	value
	μ	Kg/m.s	2.59599E-06
	M	1/n	19.562
	γ	-	1.1463
	C_p	KJ/Kg.K	4.9643
wall	k	w/m.k	13.3
Could fluid (CH4 at 111 K)	μ	Kg/m.s	0.0001213
	μ_w	m^2/s	2.86E-07
	K	w/m.k	0.1841
	C_p	KJ/Kg.K	2.232

Table 1.6: heat transfer distribution

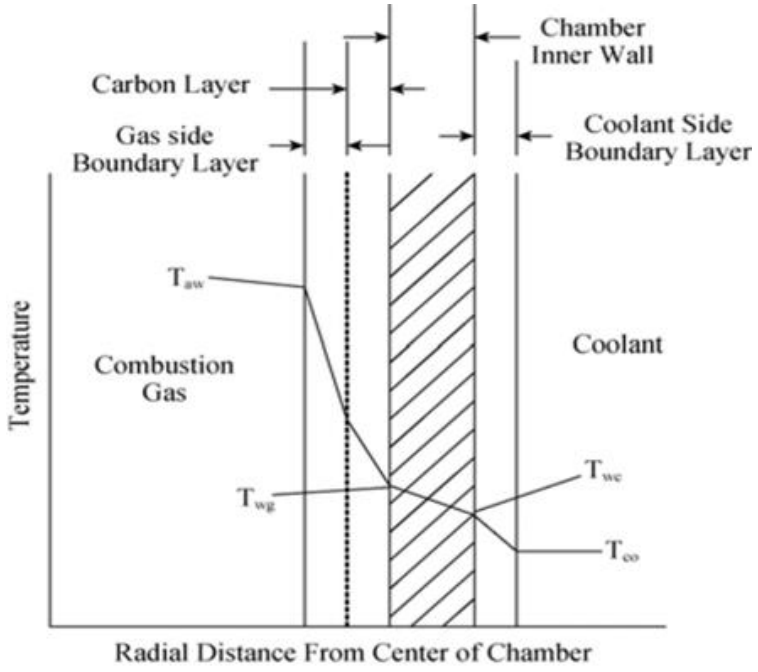

Fig 1.6: bulk temperature distribution

Parameter	**Unit**	**value**
Number of tube shell	-	35-60
Thickness of tube shell	mm	0.5
Dimeter of channel	cm	1
pressure drop in the channel	bar	

Table 1.7: Cooling Jacket Geometry

IV. Injectors

Propellant injectors considered here are limited to those which inject the propellant into the chamber as liquid jets, sheets or sprays. Mechanical adjustments and flow schemes for performing throttling functions as the manifolding can affect the start and shutdown transients (rate and evenness of flow transients) as well as the hydraulic character of the atomized sprays (different cross-velocities and inlet pressures at the upstream of the elements). The most basic rule for choosing an injector is whether or not the design supplies propellant in the manner required for highly efficient, throttling capabilities, stable and reliable operation of the combustion chamber. (11)

pintle injector

The pintle injector has been proven to be amazingly flexible and adaptable across a wide range of conditions. Pintle injectors are well known for their deep throttling capabilities, low cost compared to impinging type injectors, and high combustion efficiency. Pintle injectors typically deliver high combustion efficiency in the range of 96-99%1. Deep throttling is done using an actuation mechanism that displaces the sleeve of the pintle post axially. This displacement increases or decreases the flow of both propellants into the chamber (12). A key advantage of the pintle injector to note is its resistance to combustion instabilities partially due to resulting toroidal zones shown in Figure 1.9. These zones act as propellant rich zones that mixes and deflects unburned droplets, and cools the injector face via evaporation of impinging droplets of liquid propellant1. These recirculation zones act as dampeners for any high combustion instabilities within the chamber. Although research states this, there is no hard data shared publicly on a LRE pintle injector using a propellant combination of liquid methane and liquid oxygen. (13)

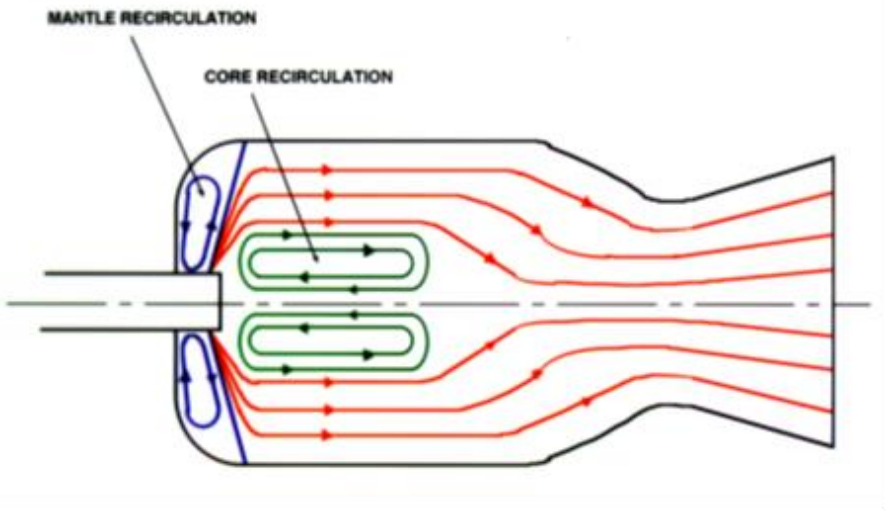

Fig 1.9: Resulting Toroidal Zones (12)

CFD analysis

injector flow field investigation of the nozzle has to be studied. A 2-D axis symmetric computational simulation of the flow field is necessary, which may be either developing a code or by using commercial code. In the present study computation has been made to obtain flow through the nozzle using commercial software ANSYS fluent axis symmetric computational simulation of the flow field. Numerical methodology with non-premixed chemical equilibrium model with assumed PDF approach is used.

Spray angle:

It is the angle formed by the cone of the liquid leaving a nozzle orifice. The spray angle is expected to stay steady all through the whole spray distance. Spray angles are directly influenced by the TMR's. As per the observations, a higher spray angle generates a uniform combustion field where every antinode is being sufficed with enough energy. Hence the possibility of combustion instability is less. (14)

Total Momentum Ratios:

TMR is the ratio between the momentum of the oxidizer to that of the sum of the momentum of the propellants. (14) The momentum of the injector's resultant spray "fan" of mixing and combusting propellants pumps two major zones of recirculation within the combustion chamber, as indicated in Figure 2.1. There is: (1) an upper torroidal zone that is predominantly outer propellant-rich and acts to cool the headend via evaporation of entrained and impinging droplets of liquid propellant, and (2) a lower toroidal zone that is predominately central propellant-rich and recirculates back on-axis toward the pintle, thereby acting as a deflector and mixer for any unburned droplets that would otherwise tend to travel directly from the injector to the nozzle throat

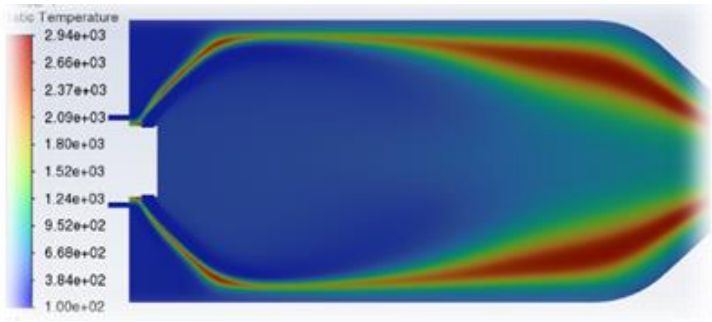

Fig 2.1: result of CFD with 90 deg LOX flow

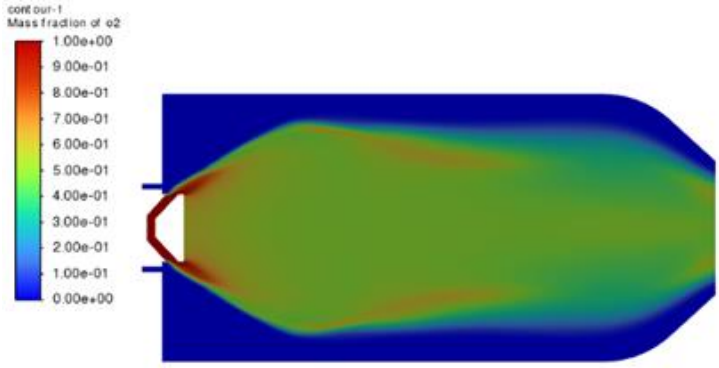

Fig 2.2: result of CFD with 47 deg LOX flow

Sauter mean diameter (SMD):

In fluid dynamics, Sauter mean diameter is an average of particle size. It is defined as the diameter of a sphere that has the same volume or surface area ratio as a particle of interest. SMD are highly impacted by the weber number, pintle angle and Lopen. The weber number has to be maintained high to procure a very fine spray. The relative velocities for

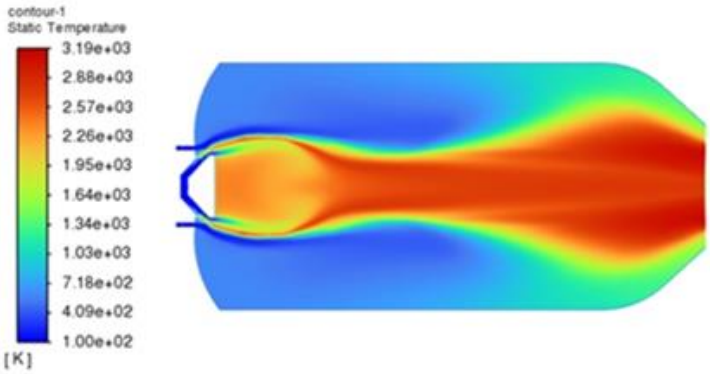

Fig 2.3: result of CFD with 47 deg LOX flow, Injector Faceplate concave

pintle injector design:
To start the design, engines requirements are to be used as input parameters. Thrust, chamber pressure, propellants, oxidizer and fuel injection temperatures, throttle capability, O/F ratio range to be observed are given as inputs. Thickness of annular gap and actual opening distance (13), which are shows in table 1.8 and fig 2.4, are the output of the design code. The discharge coefficient can be computed using the reference (13) and for future work will be revaluated by Cold Fire test.

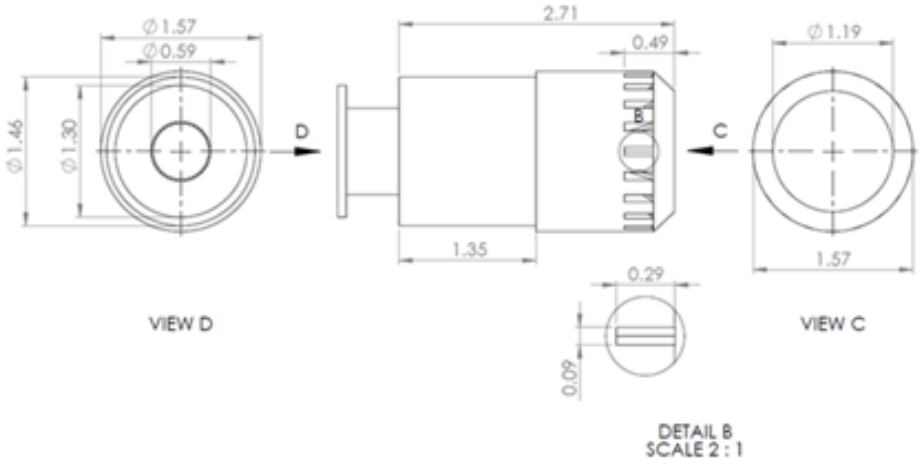

Fig 2.4: Pintle Tip dimension in centimetre

Parameter	unit	LO2	CH4
injection temperatures	K	90	161
mass flow rate	kg/s	8.096	2.89
density	Kg/m^3	1175.3	436
pressure drop %	-	20	20
discharge coefficient	-	0.65	0.75
V	m/s	31.95	60.578
Number (n)	-	20	20
flow area (A)	m2	0.02	0.0136
angle flow	deg	47	0
A/n	m^2	1.6583E-5	7.2985E-6
X	m	0.0022	
y	m	0.00744	0.00327

Table 1.8: pintle injector design parameter

Injector Mechanical Design:
At the outset of the design effort, a goal was established to evolve a configuration which would incorporate maximum flexibility as well as economy in fabrication. The basic injector concept permits adjusting both the fuel and oxidizer injection flow areas, either separately or simultaneously, thus providing increased flexibility during the initial screening phase. The design of injector consists of 4 basic parts as indicated in Figure 2.5.

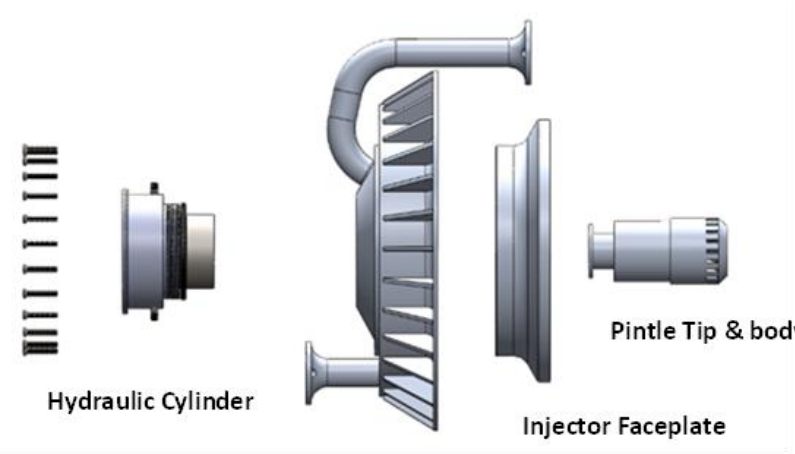

Fig 2.5: side view of injector parts

On a typical pintle injector, as a version is shown in Fig 2.6, Liquid Oxygen propellants enters the injector from the upper part, flows down inside the pintle and is ejected through a set of calibrated orifices located at the pintle tip. The hot Liquid Methane propellant enters the injector laterally and is directed into a toroidal chamber, pass through an orifice plate responsible for distributing the propellant evenly across the lower chamber, before reaching the combustion chamber in the format of a thin sheet attached to the surface of the pintle. Collisions between the radial and the axial flow stream result in the appropriated mixing and atomization. Deep throttling is done using an actuation mechanism that displaces the sleeve of the pintle post axially. This displacement increases or decreases the flow of both propellants into the chamber as the fig 2.7 shows. The sleeve is connecting with hydraulic cylinder to adjusting displacement.

Fig 2.7: actuation mechanism (sleeve)

V. Intermediate Frequency Instabilities:

Intermediate frequencies range can range from approximately 400 – 1000 Hz. This range is also known as buzzing. If not managed appropriately these instabilities can grow into high frequency instabilities. This is a secondary effect of poor injector design. A major driving mechanism for intermediate frequency instabilities is coupling with the feed system. However, they can be tied to the injection as well. Consensus for these types of instabilities states that if low frequency instabilities are managed with good pressure feed system and injector design, the absorber design can focus on high frequency instabilities (12)

VI. Material and fabrication prosses:

It's important to the material and fabrication prosses depend on the specific requirements and conditions of the rocket engine, and the injector design should be optimized accordingly.

316 stainless steel is often used in rocket engine components because it is a high-strength, corrosion-resistant alloy. It is able to withstand the high temperatures and pressures found in a rocket engine and it can also resist the corrosive effects of rocket fuel. Additionally, 316 stainless steels have excellent machinability, which makes it easy to work with during the manufacturing process. is a commonly used material in metal 3D printing because of its high strength and corrosion resistance. However, the specific process used to 3D print with 316 stainless steels will depend on the type of AM technology being used (e.g., powder bed fusion, binder jetting, etc.). Additionally, the properties of the final printed parts may be influenced by the specific process and post-processing used, and may not be identical to those of conventionally manufactured parts made from 316 stainless steel.

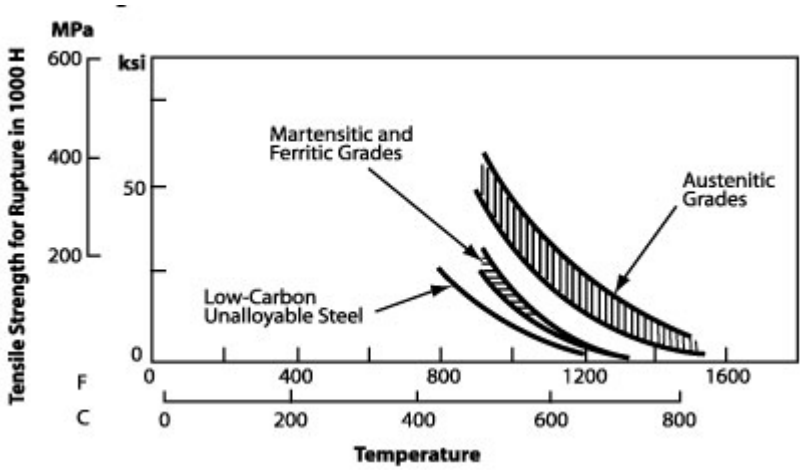

Chart 1.3: High Temperature Properties Stainless Steel

Copper alloys are used in the injectors of rocket engines for the same reasons that copper is used, but with added benefits. Copper alloys are a combination of copper and one or more other metals, such as tungsten, silver, and nickel. The addition of these other metals improves the properties of copper and makes it more suitable for use in a rocket engine injector.

- High thermal conductivity: Copper alloys have a high thermal conductivity, which allows them to dissipate heat quickly and efficiently. This is important for the injector, as it can experience high temperatures during operation.
- Good corrosion resistance: Copper alloys have good resistance to corrosion, which helps to protect the injector from degradation over time.
- Low melting point: Copper alloys have a low melting point, which makes it easier to manufacture and shape into the desired injector design.
- Durability: Copper alloys are relatively durable materials, which helps to ensure that the injector can withstand the mechanical stresses and vibration that it will experience during operation.
- High strength: Copper alloys are stronger than pure copper, which makes them more suitable for use in a rocket engine injector.
- Wear resistance: Copper alloys have better wear resistance than pure copper, which makes them suitable for use in a rocket engine injector.
- Low cost: Copper alloys are relatively low-cost materials, which makes them an economical choice for the injector of rocket engine.
- Better performance: Copper alloys can have better performance than pure copper under certain conditions, such as high temperatures, pressures, and corrosive environments.

copper alloys can be used in additive manufacturing, also known as 3D printing. Copper alloys are commonly used in various manufacturing processes including powder bed fusion, binder jetting, and Directed Energy Deposition (DED). Powder bed fusion, for example, is a process where a laser is used to melt metal powder layer by layer to create a three-dimensional object. Copper alloys can be used as the metal powder in this process, and the finished product will have the same properties as a conventionally manufactured object.

Additive manufacturing and CNC milling are popular methods used to produce these components, as they allow for precision and intricate shapes to be achieved. The use of these materials and manufacturing techniques in the design of rocket engine components is essential to ensuring the performance, reliability, and efficiency of these engines.as show in table the mines part and fabrication prosses followed for etch of them:

Mine Part		Material	Fabrication
Nozzle		316 Stainless steels	Additive Manufacturing
Combustion Chamber		316 Stainless steels	Additive Manufacturing
Manifold		316 Stainless steels	Additive Manufacturing
Pintle Injector	Pintle Tip	Copper	Additive Manufacturing
	Injector Faceplate	Copper	Machining (CNC Milling)
	Injector Body	Stainless steel	Machining (CNC Milling)
Hydraulic Cylinder	Movable Sleeve	Stainless steel	Machining (CNC Lathe)
	Cylindrical Tube	Stainless steel	Machining (CNC Lathe)
	Piston	Stainless steel	Machining (CNC Lathe)
	Base & Cap	Stainless steel	Machining (CNC Lathe)

Table 1.8: manufacturing techniques

2. Theory and calculation

The concept of ideal rocket propulsion systems is useful because the relevant basic thermodynamic principles can be expressed as simple mathematical relationships, which are given in subsequent sections of this section. An ideal rocket unit is one for which the following assumptions are valid:

- The working substance (or chemical reaction products) is homogeneous.
- All the species of the working fluid are gaseous. Any condensed phases add a negligible amount to the total mass.
- The working substance obeys the perfect gas law.
- There is no heat transfer across the rocket walls; therefore, the flow is adiabatic.
- There is no appreciable friction and all boundary layer effects are neglected.
- There are no shock waves or discontinuities in the nozzle flow.
- The propellant flow is steady and constant. The expansion of the working fluid is uniform and steady, without vibration. Transient effects are of very short duration and may be neglected.
- All exhaust gases leaving the rocket have an axially directed velocity.
- The gas velocity, pressure, temperature, and density are all uniform across any section normal to the nozzle axis.
- Chemical equilibrium is established within the rocket chamber and the gas composition does not change in the nozzle (frozen flow).
- Stored propellants are at room temperature. Cryogenic propellants are at their boiling points.

These assumptions permit the derivation of a simple, quasi-one-dimensional theory as developed in subsequent sections. **Etc.**

a. Thrust

The thrust of a rocket engine is the force generated by the propulsion system that propels the rocket in the opposite direction to the exhaust gases. The thrust of a rocket engine can be calculated using the following equation:

$$\epsilon = {}^{A_e}/_{At}$$

$$R_e = \sqrt{\epsilon}\, R_t$$

$$F = C_f P_c \pi \left(R_e / \sqrt{\epsilon}\right)^2$$
$$F = 1.53 \times 4000000\pi \left(0.12 / \sqrt{6.1}\right)^2 = 31\ KN$$

The thrust coefficient, Cf, is a dimensionless number that represents the efficiency of the nozzle in converting the internal energy of the combustion gases into kinetic energy of the exhaust gases. It depends on the nozzle design, the thermodynamic conditions of the combustion gases and the nozzle geometry (e.g. the area ratio and the expansion ratio).

b. specific volume

The specific volume in a rocket engine refers to the volume per unit mass of a substance. It is typically measured in cubic meters per kilogram (m^3/kg) or cubic feet per pound (ft^3/lb). Specific volume is an inverse of density.

In a rocket engine, specific volume is an important parameter that affects the performance of the combustion chamber and nozzle. The specific volume of the gases in the combustion chamber is determined by the properties of the propellant and the combustion process. The specific volume of the gases in the nozzle is affected by the expansion of the gases as they pass through the nozzle, which can result in significant changes in pressure and temperature. In rocket engine design, the specific volume of the gases at the nozzle exit is used to determine thrust and specific impulse (Isp) generated by the engine. The ideal specific volume for maximum thrust is the throat area of the nozzle, where the pressure is the highest. For specific impulse, the ideal specific volume is the area where the pressure has dropped to the ambient pressure.

$$R = 434.19$$
$$V_c = RT_c / P_c$$
$$V_c = 434.19 \times 3359 / 4000000 = 0.353\ m^3/Kg$$
$$V_t = V_c \left(\gamma + 1 / 2\right)^{1/(\gamma+1)}$$
$$V_t = 0.353 \left(1.2 + 1 / 2\right)^{1/(1.2+1)} \text{Kg} = 0.568\ m^3/Kg$$
$$V_e = V_c \left(P_c / P_e\right)^{1/\gamma}$$
$$V_e = 0.353 \left(4000000 / 100000\right)^{1/1.2} = 7.57\, m^3/Kg$$

c. Exit gas speed

The exit gas speed in a rocket engine is the velocity at which the exhaust gases are expelled from the nozzle. This speed is determined by the pressure and temperature of the gases in the combustion chamber, as well as the nozzle design. The ideal exit gas speed is the speed of sound in the combustion chamber gases, which is known as the sonic velocity. This ensures that the maximum amount of energy is extracted from the gases, resulting in the highest possible thrust.

$$C = C * C_f$$
$$C = 1873.9 \times 1.53 = 2847.9\ m/s$$
$$C = V_e = 2847.9\ m/s$$

d. Mass flow rate

The mass flow rate in a rocket engine is the amount of propellant (fuel and oxidizer) that is being consumed per unit of time. The mass flow rate is typically measured in kilograms per second (kg/s) or pounds per second (lb/s). The mass flow rate is one of the key parameters that affect the performance of a rocket engine and is closely related to thrust. High mass flow rates result in higher thrust and more powerful engines. The mass flow rate is determined by the properties of the propellant and the design of the injectors, pumps, and valves that deliver the propellant to the combustion chamber. The mass flow rate is also affected by the altitude and ambient temperature, as these factors can change the density of the propellant and the performance of the injectors.

$$\dot{m} = {P_c A_t}/{C^*}$$
$$\dot{m} = {40000000 \times 0.0051}/{1873.9} = 10.8\ Kg/s$$
$$\dot{m}_o + \dot{m}_f = \dot{m}$$

e. Oxidizer mass flow rate

$$\dot{m}_o = {MR\dot{m}}/{(MR+1)}$$
$$\dot{m}_o = {2.8 \times 10.8}/{(2.8+1)}$$

f. Fuel mass flow rate

$$\dot{m}_f = {\dot{m}}/{(MR+1)}$$
$$\dot{m}_f = {10.8}/{(2.8+1)} = 2.89\ Kg/s$$

1.2 Combustion chamber design

Assumption value:

- $L^* = 1.1$

1. Chamber to throat area ratio

The chamber to throat area ratio (Ac/At) is a dimensionless parameter that describes the relationship between the cross-sectional area of the combustion chamber (Ac) and the cross-sectional area of the nozzle throat (At). It is an important parameter in rocket engine design as it affects the performance of the engine, including thrust and specific impulse. The chamber to throat area ratio can be calculated using the following equation:

$$\epsilon_c \approx \left({A_c}/{A_t}\right) \approx \left({8}/{D_t^{3/5}}\right) + 1.25$$

D_t in cm

$$\epsilon_c \approx \left({A_c}/{A_t}\right) \approx \left({8}/{8^{3/5}}\right) + 1.25 = 3.53$$
$$A_c = {0.0051}/{3.53} = 0.018\ m^2$$

This equation is based on the assumption that the combustion chamber is circular and the throat is circular and the area ratio can be calculated by dividing the area of the combustion chamber by the area of the throat.

2. Chamber volume

$$V_c = {L^*}/{A_t}$$
$$V_c = {1.1}/{0.018} = 0.00566\ m^3$$

3. Resident time of gas in chamber

The residence time of gas in the chamber is a measure of the amount of time that a gas spends inside the combustion chamber of a rocket engine before it is expelled through the nozzle. It is an important parameter in the design of rocket engines, as it affects the combustion efficiency and performance of the engine.

The residence time of gas in the chamber can be calculated using the following equation:

$$t_s = {V_c}/{\dot{m} v_e}$$
$$t_s = {0.0056}/{10.9 \times 2872.6} = 0.0000017\ s$$

4. Chamber length

The chamber length in a rocket engine refers to the distance between the throat of the nozzle and the combustion chamber end. It is an important design parameter for rocket engines because it affects the performance of the

engine. In general, a longer chamber length will result in a higher specific impulse (Isp), which is a measure of the efficiency of the engine. This is because a longer chamber length allows for more complete combustion of the propellant, which results in a higher exhaust velocity and a higher thrust-to-weight ratio. However, a longer chamber length also increases the size and weight of the engine, which can be a drawback for some applications.

$$L_c = \frac{V_c - \left({}^{r_c - r_t}/_{\tan\theta}\right)A_c}{\left(1 + \sqrt{{}^{1}/_{\epsilon_c}} + {}^{1}/_{\epsilon_c}\right)A_c}$$

$$L_c = \frac{0.00566 - \left({}^{0.076 - 0.04}/_{\tan 45}\right)0.018}{\left(1 + \sqrt{{}^{1}/_{3.53}} + {}^{1}/_{3.53}\right)0.018} = 0.28\ m$$

1.5 pintle injector design

Assumption value:

- $Cd_o = 0.65$
- $Cd_o = 0.75$
- $\Delta P = 20\%$
- $n = 20$
- Loben = 0.03

1. Dimeter of O/F inject

$$d_o = \sqrt{4\dot{m}_o/\left(\pi C d_o \sqrt{2\rho\Delta P}\right)}$$

$$d_o = \sqrt{4 \times 8.09/\left(\pi \times 0.65\sqrt{2 \times 1175.3 \times 600000}\right)} = 0.02m$$

$$d_f = \sqrt{4\dot{m}_f/\left(\pi C d_f \sqrt{2\rho\Delta P}\right)}$$

$$d_f = \sqrt{4 \times 2.89/\left(\pi \times 0.75\sqrt{2 \times 436 \times 800000}\right)} = 0.013m$$

2. Ratio of flow area to injection area number

The ratio of flow area to injection area number (A/n) in a pintle injector refers to the proportion of the cross-sectional area of the flow channel, compared to the cross-sectional area of the injection hole(s) in the injector face. This ratio is important in determining the mixing characteristics of the injected fluid and combustion efficiency in a rocket engine. A high A/n ratio can result in inefficient mixing, leading to incomplete combustion, while a low A/n ratio can result in increased pressure drop and reduced performance. The optimal A/n ratio for a pintle injector depends on various factors such as the injector design, combustion chamber pressure, and fluid properties, and is usually determined through experimentation and numerical simulations.

$${A_o}/_{n} = {0.00033}/_{20} = 0.0000016\ m^2$$

$${A_f}/_{n} = {0.00033}/_{20} = 0.000000017\ m^2$$

3. Inject speed

The Injector Speed Equation is a mathematical model that describes the relationship between the mass flow rate of the propellant, the velocity of the propellant, and the geometry of the injector orifices. The injector speed equation is an important tool for designing and analysing rocket engine injectors.

$$v_o = {2\Delta p}/{\rho}$$

$$v_o = {2 \times 600000}/{1175.3} = 31.9\ m/s$$

$$v_f = {2\Delta p}/{\rho}$$

$$v_f = {}^{2 \times 800000}/_{436} = 60.5\ m/s$$

4. Total Momentum Ratios

   The Total Momentum Ratio (TMR) is a dimensionless number that is used to quantify the performance of a rocket nozzle. It is defined as the ratio of the total momentum of the exhaust gases at the nozzle exit plane to the total momentum of the propellant at the nozzle throat. The TMR equation is given by:

$$TMR = \frac{(mv)_o \sin\theta}{(mv)_o \sin\theta + (mv)_f}$$
$$TMR = \frac{(8.09 \times 31)\sin 47}{(8.09 \times 31)\sin 47 + (2.89 \times 61)} = 0.5$$
$$\alpha = \cos^{-1}\left({}^{1}/_{1+TMR}\right)$$
$$\alpha = \cos^{-1}\left({}^{1}/_{1+0.5}\right) = 48\text{deg}$$

   The TMR is a measure of the efficiency of the nozzle in converting the kinetic energy of the propellant into the kinetic energy of the exhaust gases. A higher TMR value indicates a more efficient nozzle, as it means that more of the propellant's kinetic energy is being converted into the kinetic energy of the exhaust gases, which results in a higher thrust.

1.3 steady-state one-dimensional heat transfer equations

Steady-state one-dimensional heat transfer equations describe the heat transfer that occurs in a rocket engine under steady-state conditions, where the temperature and heat flow are constant over time. These equations take into account the heat generated by combustion and the heat transferred to the walls of the engine, as well as the heat lost through the exhaust. They can be used to determine the temperature distribution and heat loss within the engine, and can also be used to design cooling systems for the engine. The equations are typically solved using numerical methods such as finite difference or finite element analysis. regenerative cooling analyses were performed for a number of cases using a computer program developed in MATLAB (Appendix A (MATLAB code)). This computer program solves the steady-state one-dimensional heat transfer equations. and is capable of either designing or evaluating channel wall coolant passages in different configurations. The Program output includes coolant heat input, coolant pressure and bulk temperature distribution and chamber wall temperature profiles.

The general steady-state heat transfer equations for regeneratively cooled thrust chambers can be expressed as follows:

1. Coefficient of Heat Transfer gas said

   The coefficient of heat transfer (h) in a rocket engine refers to the rate of heat transfer per unit area per unit temperature difference between the fluid (such as coolant or propellant) and the wall of the engine. It is often used in calculations related to heat transfer in the engine, such as determining the heat transfer rate or the temperature distribution of the fluid. The value of h is dependent on the fluid properties, velocity, and the surface characteristics of the engine. It can be calculated using various heat transfer correlations.

$$P_r = \frac{4\gamma}{9\gamma - 5}$$
$$\mu = 46.6 \times 10^{-10} M^{0.5} T^{0.6}$$
$$h_g = \left[\frac{0.026}{D_t^{0.2}} \frac{\mu^{0.2} C_p}{P_r^{0.6}} \left(\frac{P_c}{C^*}\right)^{0.8} \left(\frac{D_t}{R}\right)^{0.1}\right] \left(\frac{A_t}{R}\right)^{0.9} \sigma$$
$$h_{gc} = \frac{1}{\left({}^{1}/_{h_g}\right) + R_c}$$
$$h_g = h_{gc} \rightarrow by\ assume\ no\ carbon\ deposit$$

2. Adiabatic flame Temperature

Adiabatic flame temperature (AFT) is the theoretical temperature that a combustion reaction would reach if the combustion process were to occur under adiabatic conditions. Adiabatic conditions refer to a process that occurs without the transfer of heat or matter to or from the system. It is the highest temperature that can be achieved in a combustion process and it is dependent on the chemical composition of the combustion products and the initial reactants. It is a measure of the potential energy available in the combustion process. Adiabatic flame temperature is an important parameter in rocket engine combustion design, as high AFTs can lead to higher performance and specific impulse. In rocket engines, the combustion process usually occurs at high pressure, high temperature and high velocity, the equation that is commonly used to calculate the adiabatic flame temperature is the thermochemical equilibrium equations which consider the thermodynamic properties of the combustion products, the initial reactants and the combustion products, and the initial conditions of pressure and temperature.

In general, the adiabatic flame temperature is calculated using the following equation:

$$T_{aw} = T_c \left[\frac{1 + r\left(\gamma - {}^{1}/_{2}\right) M_x^2}{1 + \left(\gamma - {}^{1}/_{2}\right) M_x^2} \right]$$

3. Conductive heat transfer

Conductive heat transfer, also known as conduction, is the transfer of heat energy through a solid material by the collision of atoms and molecules. In a rocket engine, conductive heat transfer occurs primarily through the walls of the combustion chamber and nozzle. The heat generated by combustion is conducted through the walls of the chamber and nozzle to the coolant fluid, which is responsible for removing the heat and maintaining the structural integrity of the engine.

Conductive heat transfer is governed by the equation:

$$q = h_g \left(T_{ag} - T_{wg} \right)$$
$$T_{wc} = \frac{q + h_c T_{co}}{h_c}$$

Conductive heat transfer is an important aspect of rocket engine design, as it directly impacts the structural integrity of the engine and the cooling performance. The heat transfer coefficient, thermal conductivity, and temperature range of the materials used in the combustion chamber and nozzle walls are carefully selected and optimized to ensure safe and efficient operation of the engine.

4. Coefficient of Heat Transfer wall said

$$h_w = \frac{K_w}{t_w}$$

5. Coefficient of Heat Transfer fluid said relation

Equation (1)

$$h_c = \left[\frac{0.029\, C_p\, \mu^{0.2}}{\left(\frac{\mu\, C_P}{K}\right)^{2/3}} \right] \left[\frac{\left(\frac{4\dot{\omega}_f}{\pi\, N\, d^2}\right)^{0.8}}{d^{0.2}} \right] \left(\frac{T_{co}}{T_{wc}}\right)^{0.55}$$

Equation (2)

$$\frac{h_c d}{K} = C_1 \left[\frac{\rho \left[\frac{\dot{\omega}_f}{\rho} \Big/ \left(\frac{N}{2} \frac{\pi d^2}{4} \right) \right] d}{\mu} \right]^{0.8} \left(\frac{\mu C_P}{K}\right)^{0.4} \left(\frac{\mu}{\mu_w}\right)^{0.14}$$

5. Results

Based on the previous summary of the design for a reusable rocket liquid oxygen/methane thrust chamber, it appears that the initial design satisfies the technical specifications outlined as follow:

Parameter	Unit	Value
Thrust	KN	31
Chamber Pressure	Bar	40
Operation Pressure	Bar	1.0132
Mixture Ratio	-	2.8
Flue	K	110
oxidizer	K	90
Mass Flow Rate	Kg/s	10.98
Chamber Temperature	K	3359.1
Specific Impulse	s	2872.7
Frequency Instabilities	Hz	
Engine Mass	Kg	25.596
Thrust To Weight Eng Ratio	-	124
Engine Length	m	0.93
Engine Dimeter	m	0.3

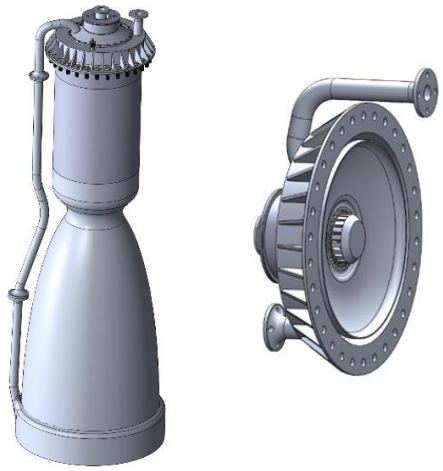

Mine Part		Material	Fabrication
Nozzle		316 Stainless steels	Additive Manufacturing
Combustion Chamber		316 Stainless steels	Additive Manufacturing
Manifold		316 Stainless steels	Additive Manufacturing
Pintle Injector	Pintle Tip	Copper	Additive Manufacturing
	Injector Faceplate	Copper	Machining (CNC Milling)
	Injector Body	Stainless steel	Machining (CNC Milling)
Hydraulic Cylinder	Movable Sleeve	Stainless steel	Machining (CNC Lathe)
	Cylindrical Tube	Stainless steel	Machining (CNC Lathe)
	Piston	Stainless steel	Machining (CNC Lathe)
	Base & Cap	Stainless steel	Machining (CNC Lathe)

6. Discussion

The design of a reusable rocket engine is a complex process that requires a deep understanding of various technical aspects such as heat transfer, fluid dynamics, and thermodynamics. Despite the advancements made in this field, there is still a significant scope for improvement and further optimization. The discussion of the design of a reusable rocket engine in this paper highlights the current state of the art and identifies areas for further research. The focus is on exploring the strengths and weaknesses of existing designs and making recommendations for future work. The goal is to provide a comprehensive analysis of the current state of the field and offer insights into how to improve the efficiency and reliability of reusable rocket engines. With the increasing demand for long-duration missions and landing impacts on Mars, it is crucial to identify the challenges faced by current designs and develop innovative solutions. By doing so, the paper aims to contribute to the development of more advanced and efficient reusable rocket engines.

Additional recommendations for future works:

- Work on Hot & Cold fire test to analysis and evaluate the Characteristic length, discharge coefficient, Coolant inlet fuel Temperature and Carbon deposit factor to redesign rocket for more performance.
- Design Electric Feed Systems for Liquid Propellant Rocket Engines
- The next highly interesting investigation focus lies on the demonstration of the so-called injection-cooling method and flame cooling method. More detailed numerical simulations of mixing and combustion will be performed to increaser reusability of the engine.

- Numerical simulations on internal flows were conducted to estimate the fuel distributions and associated pressure losses in the feed lines for each propellant.
- Cold flow tests for each propellant showed a good agreement between numerical and experimentally measured data.
- Final hot firing tests confirmed a good performance for both mixing and cooling techniques.
- Work on Engine cycle, Retro-Propulsion system and Propulsion feed system and thermal isolation of critical structures.
- drawings have been completed, and will be updated to changes need to be done to the design following the reviews and to some solve technical problems.
- Manufacturing and associated modifications to be full rocket engine 3D printing.
- provide the foundations and the physical understanding for the application of technologies for retro propulsion assisted landing.
- investigate the thermal loads of a re-usable first stage during the retro-propulsion maneuver and the final landing approach using simulations program.

6. Conclusions

From the previous summary about the design of a reusable rocket liquid oxygen/Methane thrust chamber, it can be concluded that such preliminary design meets the requirements of the technical specification for development and operation of Reusable landing and take-off. Engine provide high specific impulse which is suitable for use in rocket upper and booster stages. For the thrust chamber modelled at 31KN of thrust and chamber pressure of 40 bar with the Thrust to Weight Engen Ratio of 124 shows a very good consistency when compared with computational results. Those results, with the associated design and modelling tools maturation, pave the way to a lower risk application of the studied Engine and Rocket Propulsion System for innovative reusable rocket Engen projects that are burgeoning, in particular for re-usable launcher stages, among others.

Acknowledgements

I am grateful to the International Conference on Space Operations and the Mohammed Bin Rashid Space Centre (MBRSC) for providing me with the opportunity to present my research paper. This platform has been instrumental in bringing together experts in the field of space operations and has provided me with a unique opportunity to share my ideas and receive valuable feedback.

I would also like to express my gratitude to the organizing committee for their efforts in making this event a success. Their dedication and hard work have created a vibrant and engaging atmosphere, where ideas can be freely exchanged and discussed.

Finally, I would like to thank my colleagues, friends, and family for their unwavering support throughout this process. Their encouragement and motivation have been invaluable and have allowed me to reach this point.

This has been an incredible experience, and I am grateful for the opportunity to be a part of it.

Appendix A (MATLAB code)

1. Solve steady-state one-dimensional heat transfer equations & coolant passages

```
clear all
clc
%%gas said calculation
Rd=0
y=1.2
M=19.6
T=3132
Aratio=1
rt=0.04
Dt=0.08
```

```
Te=2021
Cp=4.7
Pc=4*10^6
Cstar=1861
Tc=3329
De=0.2
Me=2.6

%--------------%
%Wall material calculation
Twg=600 %assuming -----important facture**
t=0.001 % thickens of inner tube shell --- important facture**
k=27.7 %from W/M.s to But/s.in.F
Kf=0.1307
%---------------%
% Fluid cooling data
uw=0.2027*10^-6
Tco=146%it is temp of inter of coolant fluid --- important facture**
Cpf_e=2
uf_e=0.0000798 %from cp to Ib/in-s
Kf=0.1307
Mx=1 %mauc number at throat where most heat transfer large
Mf= 2.9 %mass fuel rate

%%hg calculation for gas camper said
re=De/2
Pr=(4*y)/((9*y)-5)
u=(46.6*(10^-10))*(M^0.5)*(T^0.6)
R=((rt*1.5)+(rt*0.4))/2
r=Pr^0.33 % for turbulent flow
Taw=Tc*((1+(r*((y-1)/2)*(Mx^2)))/(1+(((y-1)/2)*(Mx^2))))
s=(((1/2)*(Twg/Taw)*(1+(y-1/2)*(Mx^2))+(1/2))^-0.68)*(((1+(y-1/2)*(Mx^2))+(1/2))^-
0.21)

%%at throat of Nozzle
h1=(0.026/(Dt^0.2))
h2=(((u^0.2)*Cp)/(Pr^0.6))
h3=((Pc/Cstar)^0.8)
h4=((Dt/R)^0.1)
h5=(Aratio^0.9)*s
hg=h1*h2*h3*h4*h5
hw=k/t
i=((De-Dt)/De)*100
     if i>=80
    %At exit of Nozzle
    Taw_e=Tc*((1+(r*((y-1)/2)*(Me^2)))/(1+(((y-1)/2)*(Me^2))))
hg_e1=(0.026/(Dt^0.2))
hg_e2=(((u^0.2)*Cp)/(Pr^0.6))
hg_e3=((Pc/Cstar)^0.8)
hg_e4=((Dt/1)^0.1)
hg_e5=(Aratio^0.9)*s
hg_e=hg_e1*hg_e2*hg_e3*hg_e4*hg_e5
            if Rd>=1
            hgc_e=1/((1/hg_e)+Rd);
            q_e=hgc_e*(Taw_e-Twg);
```

```
            disp(q)
            end
              if Rd==0
              q_e=hg_e*(Taw_e-Twg);
              disp(q_e)
              end
Tco_t=((q_e*((pi*re^2)-(pi*rt^2)))+(Mf*Cpf_e*Tco_e))/(Mf*Cpf_e)
fprintf('enter value could fluid at temp of',Tco_t)
Cpf_e=input('Cpf')
uf_e=input('uf')
Twc=Twg-((q_e*t)/k)
hc_e=q_e/(Twc-Tco_t)
N11=(Tco_t/Twc)^(11/16)
N12=(0.0119*(Cpf_e^1.25)*(uf_e^0.25))/(Pr^(5/6))
N13=((Mf*4)/pi)
N14=(1/hc_e)^1/0.8
Fx1=N11*N12*N13*N14

            gi=(De/2)*0.2;
           for d=0:0.000001:1

N1=Fx1*(d^-2.25);
N2=(pi*(Dt+0.8*(d+2+t)))/(d+(2*t)) ;
N3=(pi/asin(((d+t*2)/2)/(((d+t*2)/2)+(Dt/2))));
if N1>=N3 && N2>=N3
    disp(N1)
    disp(N2)
    disp(N3)
    disp(d)

end
end
              if Fx1<=0
    disp("No result of N and d ")
    disp("Rong in calculation of Cpf uf kf Tco Twc or hg")
              end
    %_____________________________%

else

if Rd>=1
      hgc=1/((1/hg)+Rd);
      q=hgc*(Taw-Twg);
      disp(q)
end
if Rd==0
    q=hg*(Taw-Twg);
    disp(q)
end
Twc=Twg-((q*t)/k)
hc=q/(Twc-Tco)

%%%%calculating Number of tube cooling and diameter
fprintf('enter value could fluid at temp of',Tco)
Cpf=input('Cpf')
```

```
uf=input('uf')
N11=(Tco/Twc)^(11/16)
N12=(0.0119*(Cpf^1.25)*(uf^0.25))/(Pr^(5/6))
N13=((Mf*4)/pi)
N14=(1/hc)^1/0.8

%Equation 2 and 1 solve
Fx1=N11*N12*N13*N14
gi=(De/2)*0.2; %limit of for
for d=0:0.000001:1

N1=Fx1*(d^-2.25);
N2=(pi*(Dt+0.8*(d+2+t)))/(d+(2*t)) ;
N3=(pi/asin(((d+t*2)/2)/(((d+t*2)/2)+(Dt/2))));
if N1>=N3 && N2>=N3
    disp(N1)
    disp(N2)
    disp(N3)
    disp(d)

end
end
if Fx1<=0
    disp("No result of N and d ")
    disp("Rong in calculation of Cpf uf kf Tco Twc or hg")
end
      end
    %-------------------------------------%
```

1. computer program solves the characteristic

```
clear all
clc
tic
%% Gas properties %%
gamma=input('Enter Cp/Cv ');
%% Design parameters %%
Me=input('Enter exit Mach no. : ');
theta_max=PrandtlMeyer(Me,gamma)*180/(2*pi);
%% Incident expansion wave conditions %%
n=input('Enter number of characteristics lines (greater than 2) emanating from
sharp corner throat : ');
theta_0=theta_max/n ;
%% Characteristic parameter solver
% v - Prandtl-Meyer function
% KL - Left running characteristic constant
% KR - Right running characteristic constant
% theta - Flow angle relative to horizontal
[v,KL,KR,theta]=moc2d(theta_max,theta_0,n);
%% Mach number and Mach angle at each node
node=0.5*n*(4+n-1);
M=zeros(1,node);
mu=zeros(1,node);
for i=1:node
    M(i)=InvPrandtlMeyer(v(i));
```

```
        mu(i)=Mu(M(i));
    end
    %% Grid generator
    figure(1)
    D=1; % Non-Dimensional y co-ordinate of throat wall
    i=1;
    x=zeros(1,node);
    y=zeros(1,node);
    wall=theta_max;
    while (i<=n+1)
        if i==1
            x(i)=-D/(tand(theta(i)-mu(i)));
            y(i)=0;
            plot([0 x(i)],[D 0]);
            hold on
        else if i==n+1
                x(i)=(y(i-1)-D-x(i-1)*tand((theta(i-1)+theta(i)+mu(i-
1)+mu(i))*0.5))/(tand(0.5*(wall+theta(i)))-tand((theta(i-1)+theta(i)+mu(i-
1)+mu(i))*0.5));
                y(i)=D+x(i)*tand(0.5*(wall+theta(i)));
                plot([x(i-1) x(i)],[y(i-1) y(i)]);
                hold on
                plot([0 x(i)],[D y(i)]);
                hold on
            else
                x(i)=(D-y(i-1)+x(i-1)*tand(0.5*(mu(i-1)+theta(i-
1)+mu(i)+theta(i))))/(tand(0.5*(mu(i-1)+theta(i-1)+mu(i)+theta(i)))-tand(theta(i)-
mu(i)));
                y(i)=tand(theta(i)-mu(i))*x(i)+D;
                plot([x(i-1) x(i)],[y(i-1) y(i)]);
                hold on
                plot([0 x(i)],[D y(i)]);
                hold  on
            end
        end
        i=i+1;
        hold on
    end
    h=i;
    k=0;
    i=h;
    for j=1:n-1
        while (i<=h+n-k-1)
            if (i==h)
                x(i)=x(i-n+k)-y(i-n+k)/(tand(0.5*(theta(i-n+k)+theta(i)-mu(i-n+k)-
mu(i))));
                y(i)=0;
                plot([x(i-n+k) x(i)],[y(i-n+k) y(i)]);
                hold on
            else if (i==h+n-k-1)
                    x(i)=(x(i-n+k)*tand(0.5*(theta(i-n+k)+theta(i)))-y(i-n+k)+y(i-1)-
x(i-1)*tand((theta(i-1)+theta(i)+mu(i-1)+mu(i))*0.5))/(tand(0.5*(theta(i-
n+k)+theta(i)))-tand((theta(i-1)+theta(i)+mu(i-1)+mu(i))*0.5));
                    y(i)=y(i-n+k)+(x(i)-x(i-n+k))*tand(0.5*(theta(i-n+k)+theta(i)));
                    plot([x(i-1) x(i)],[y(i-1) y(i)]);
```

```
                hold on
                plot([x(i-n+k) x(i)],[y(i-n+k) y(i)]);
                hold on
            else
                s1= tand(0.5*(theta(i)+theta(i-1)+mu(i)+mu(i-1)));
                s2= tand(0.5*(theta(i)+theta(i-n+k)-mu(i)-mu(i-n+k)));
                x(i)=(y(i-n+k)-y(i-1)+s1*x(i-1)-s2*x(i-n+k))/(s1-s2);
                y(i)=y(i-1)+(x(i)-x(i-1))*s1;
                plot([x(i-1) x(i)],[y(i-1) y(i)]);
                hold on
                plot([x(i-n+k) x(i)],[y(i-n+k) y(i)]);
                hold on
            end
        end
        i=i+1;
    end
    k=k+1;
    h=i;
    i=h;
    hold on
end
title(sprintf('Characteristic lines for Mach=%d and Cp/Cv=%d',Me,gamma))
xlabel('x/x0');
ylabel('y/y0');
axis equal
xlim([0 x(node)+0.5])
ylim([0 y(node)+0.5])
toc
```

Appendix B (CAD Drowning)

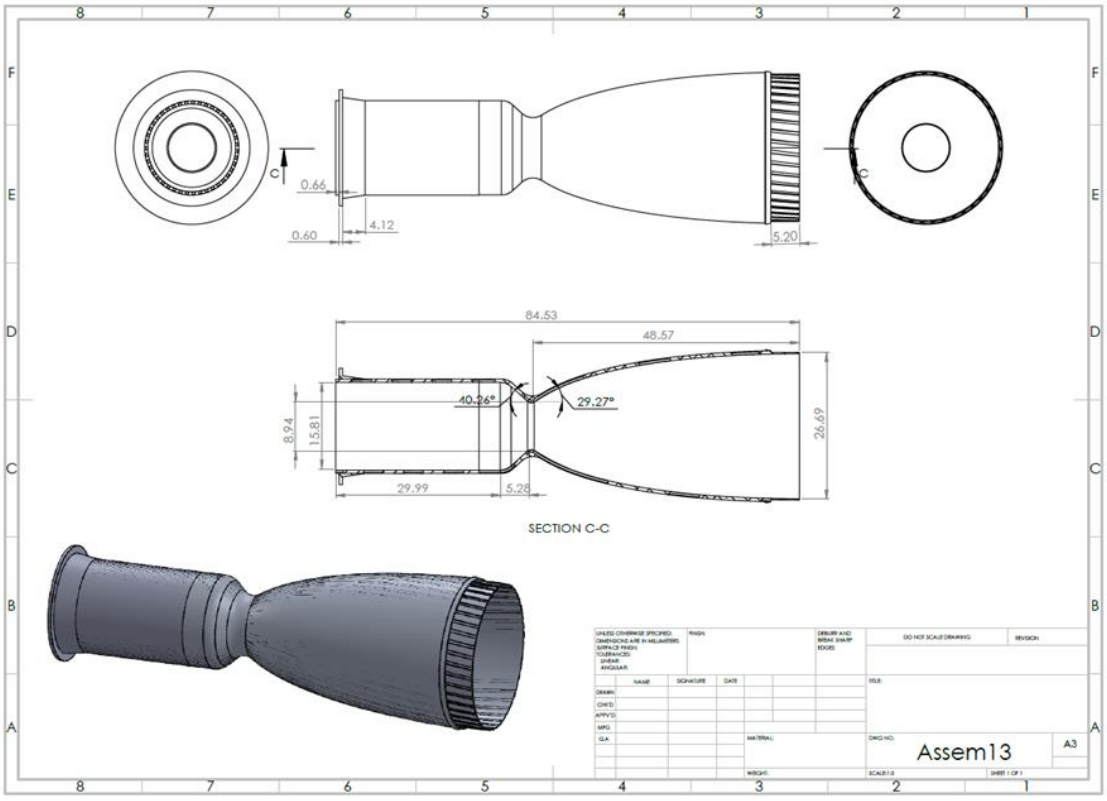

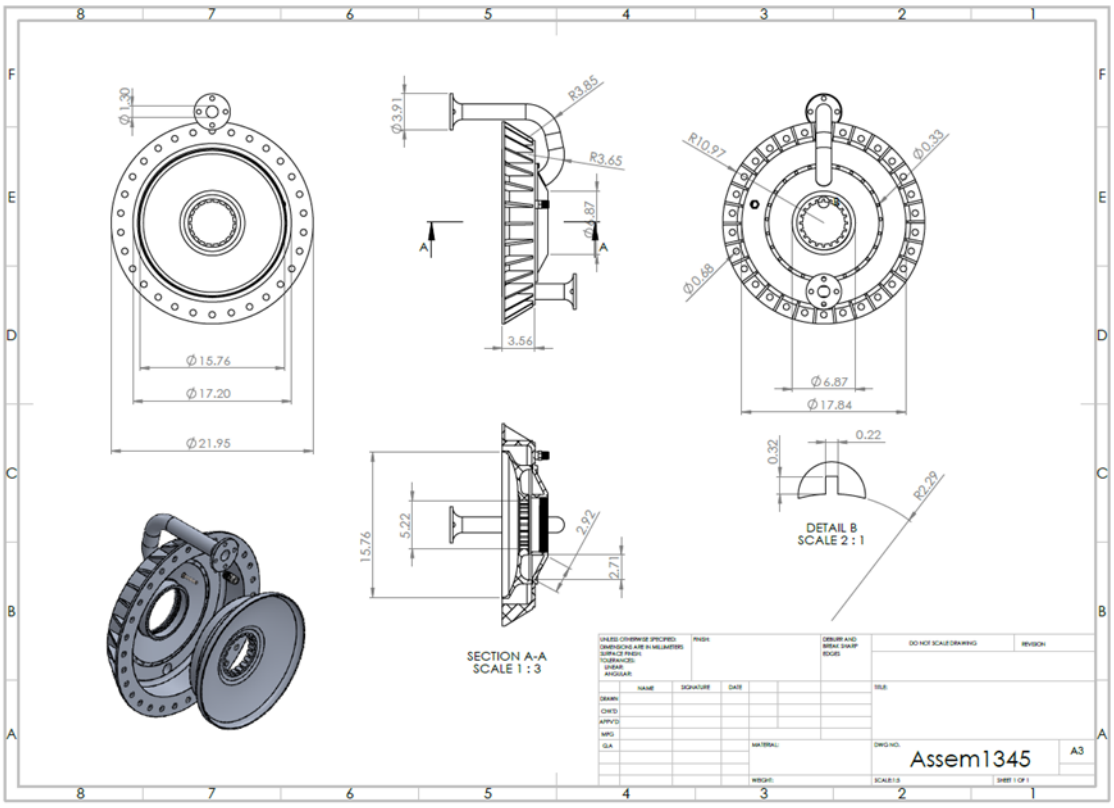

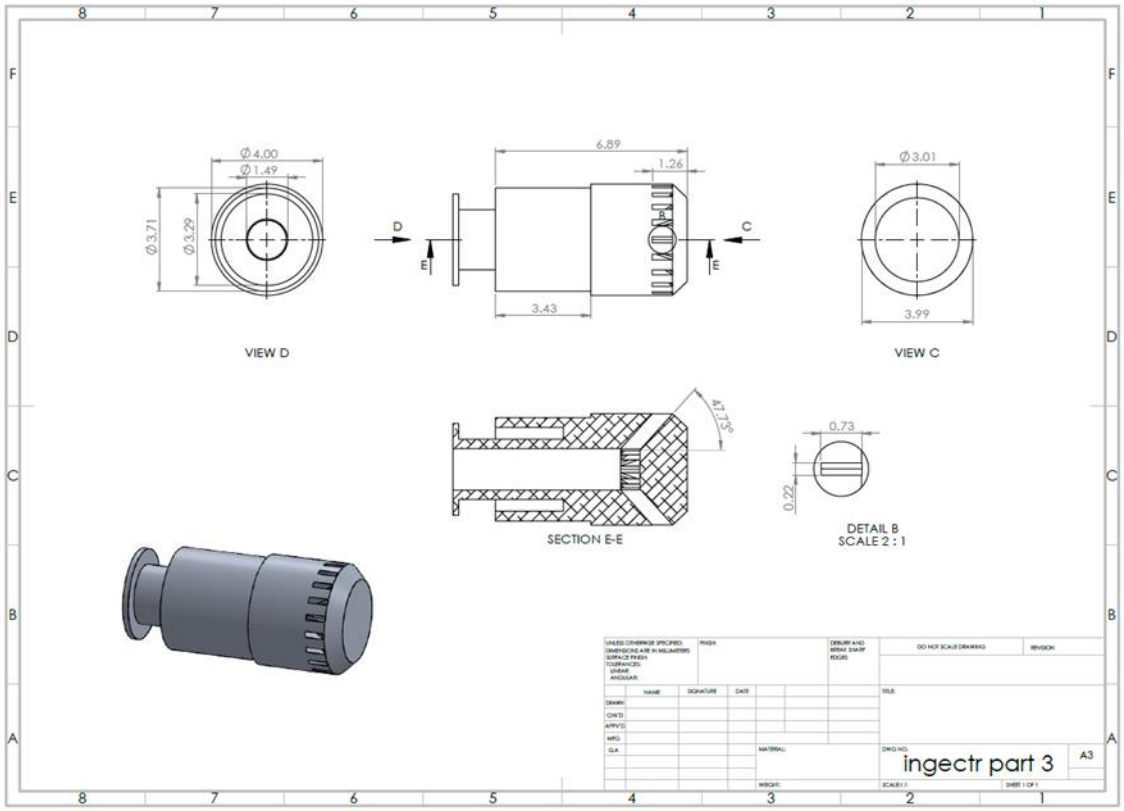

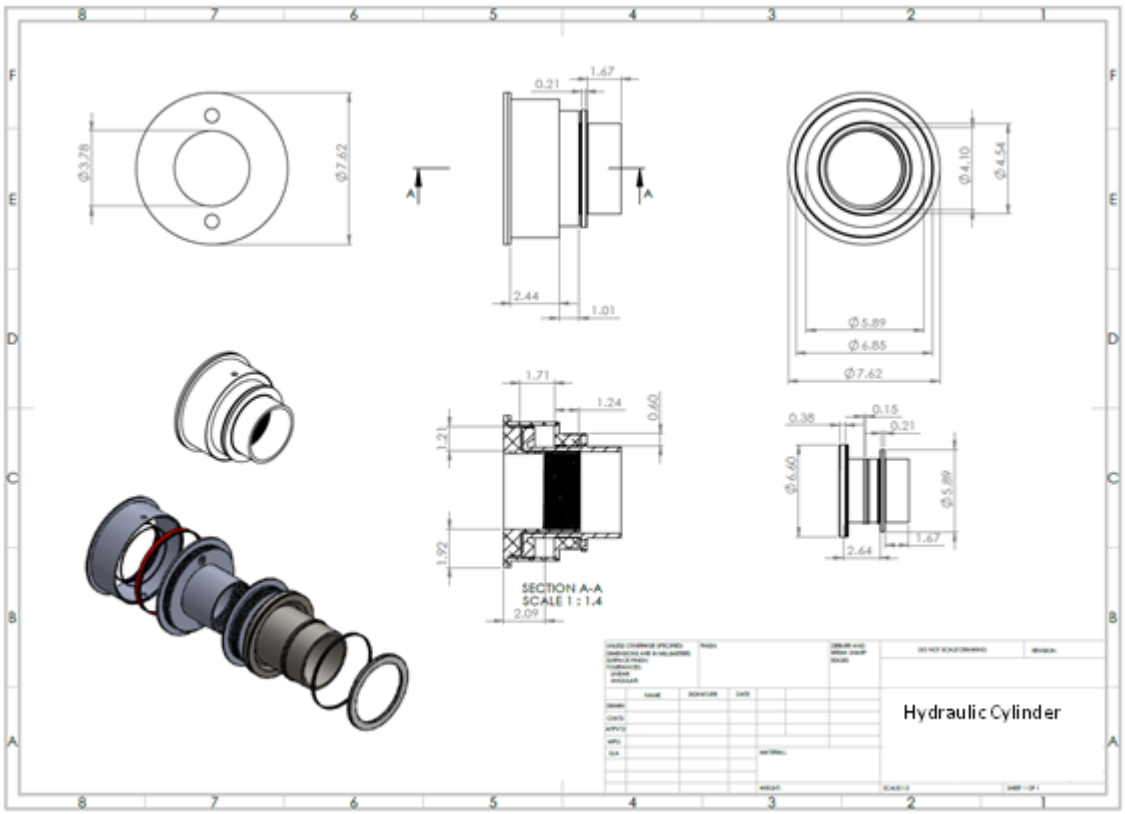

References

1. Vasques BB, Haidn OJ. Effect of Pintle Injector Element Geometry on Combustion in a Liquid Oxygen/Liquid Methane Rocket Engine. 2017;
2. Müller I, Kuhn M, Petkov I, Bletsch S, Huybrechts K, van Cauwenbergh P. 3D-PRINTED COAXIAL INJECTOR FOR A LOX/KEROSENE ROCKET ENGINE SPACE PROPULSION 2018 (6) (1)(2)(3)(4).
3. Zilker F. Aerothermal Analysis of Re-usable First Stage during Rocket Retro-propulsion. 2018.
4. Kuttan BP, Sajesh M. Optimization of Divergent Angle of a Rocket Engine Nozzle Using Computational Fluid Dynamics [Internet]. Available from: www.theijes.com
5. Kato T, Terakado D, Nanri H, Morito T, Masuda I, Asakawa H, et al. Subscale Firing Test for Regenerative Cooling LOX/Methane Rocket Engine.
6. Turner MJL. Rocket and spacecraft propulsion : principles, practice and new developments. Springer; 2005. 313.
7. Fas M. São José dos Campos, v10, e3018. Goertz. 2018.
8. IAC_17_C4_10_11_X_39688_DLR_Ortelt_Manuscript.
9. Fas M. São José dos Campos, v10, e3018. Goertz. 2018.
10. Bai MO. NUMERICAL EVALUATION OF HEAT TRANSFER AND PRESSURE DROP IN OPEN CELL FOAMS. 2007.
11. Casiano MJ, Hulka JR, Yang V. Liquid-propellant rocket engine throttling: A comprehensive review. Vol. 26, Journal of Propulsion and Power. American Institute of Aeronautics and Astronautics Inc.; 2010. p. 897–923.
12. Candelaria J. Theoretical Acoustic Absorber Design Approach for LOX/LCH4 Pintle Injector Rocket Engines.
13. Dressler GA, Martin Bauer J. TRW Pintle Engine Heritage and Performance Characteristics. 2000.
14. Yu I, Kim S, Ko Y, Kim S, Lee J, Kim H. Combustion Performance of a Pintle Injector Rocket Engine with Canted Slit Shape by Characteristic Length and Total Momentum Ratio. Journal of the Korean Society of Propulsion Engineers. 2017 Feb 1;21(1):36–43.